

ATM/ATR checkpoint activation downregulates CDC25C to prevent mitotic entry with uncapped telomeres

Maria Thanasoula¹,
Jose Miguel Escandell, Natsuko Suwaki
and Madalena Tarsounas*

Telomere and Genome Stability Group, The CR-UK/MRC Gray Institute for Radiation Oncology and Biology, Department of Oncology, University of Oxford, Oxford, UK

Shelterin component TRF2 prevents ATM activation, while POT1 represses ATR signalling at telomeres. Here, we investigate the mechanism of G2/M arrest triggered by telomeres uncapped through TRF2 or POT1 inhibition in human cells. We find that telomere damage-activated ATR and ATM phosphorylate p53, as well as CHK1 and CHK2, thus activating two independent pathways to prevent progression into mitosis with uncapped telomeres. Surprisingly, telomere damage targets the CDC25C phosphatase for proteasome degradation in G2/M. CHK1/CHK2-dependent phosphorylation of CDC25C at Ser 216 is required for CDC25C nuclear export and destruction, which in turn acts to sustain the G2/M arrest elicited by TRF2- or POT1-depleted telomeres. In addition, CDC25C is transcriptionally downregulated by p53 in response to telomere damage. These mechanisms are distinct from the canonical DNA damage response to ionizing radiation, which triggers cell-cycle arrest through CDC25A destruction. Thus, dysfunctional telomeres promote ATM/ATR-dependent degradation of CDC25C phosphatase to block mitotic entry, thereby preventing telomere dysfunction-driven genomic instability.

The EMBO Journal (2012) 31, 3398–3410. doi:10.1038/emboj.2012.191; Published online 27 July 2012

Subject Categories: genome stability & dynamics

Keywords: ATM/ATR kinases; CDC25 phosphatases; checkpoint activation; telomere

Introduction

Telomere uncapping occurs in senescent cells due to erosion of telomeric repeats or in normally growing cells due to loss of telomere protective factors (di Fagagna *et al*, 2003; Takai *et al*, 2003). This leads to checkpoint activation and telomeric accumulation of DNA damage response factors (e.g., phosphorylated histone H2AX (γ H2AX), phosphorylated

ATM, 53BP1) into microscopically defined telomere-dysfunction induced foci (TIFs; di Fagagna *et al*, 2003; Takai *et al*, 2003). Downstream signalling pathways then engage the DNA repair machinery to join unprotected telomeres into deleterious end-to-end fusions, which can lead to cell-cycle arrest or cell death. Thus, the signal emanating from dysfunctional telomeres resembles that triggered by unrepaired double-strand breaks (DSBs).

CHK1 and CHK2 kinases are key signal transducers within the network of genome integrity checkpoints (Bartek and Lukas, 2003). Following exposure to ionizing radiation (IR), ATM signalling initiates resection, which generates the single-stranded DNA substrate for replication protein A (RPA) loading. This, in turn, promotes ATR activation required for CHK1 phosphorylation (Cuadrado *et al*, 2006; Jazayeri *et al*, 2006). CHK2 is phosphorylated in an ATM- and NBS1-dependent manner (Matsuoka *et al*, 2000; Buscemi *et al*, 2001) to trigger its activation. Thereafter, CHK1 and CHK2 initiate additional phosphorylation events to complete signalling to cell-cycle effectors. During G2/M, the roles of CHK1 and CHK2 converge to phosphorylate and inactivate CDC25A and CDC25C, two members of the CDC25 dual specificity phosphatase family, with roles in driving cells through the cell cycle (Bartek and Lukas, 2003; Kastan and Bartek, 2004). These enzymes remove crucial inhibitory phosphorylations on CDK/cyclin complexes, the most important being dephosphorylation of Tyr15 in the ATP-binding loop of CDK1(CDC2) and CDK2 (Reinhardt and Yaffe, 2009).

CHK1-mediated phosphorylation of CDC25A at multiple sites is required for IR-induced G2/M checkpoint activation (Bartek and Lukas, 2007). Importantly, CHK1 phosphorylation of CDC25A at Ser76 promotes its SCF ^{β -TRCP}-dependent ubiquitylation and subsequent degradation by the proteasome (Busino *et al*, 2003). Similarly, CHK2 can phosphorylate CDC25A and CDC25C in response to DNA damage to induce G2/M cell-cycle arrest, as well as p53-dependent apoptosis (Ahn *et al*, 2004; Kastan and Bartek, 2004). CHK2 lacks the ability to phosphorylate CDC25A at Ser76 (Jin *et al*, 2008) or trigger its degradation, however, it phosphorylates CDC25C at Ser216 (Matsuoka *et al*, 1998) to facilitate the binding of 14-3-3 proteins which retain CDC25C in the cytoplasm (Peng *et al*, 1997). So far, CDC25C ubiquitylation and proteasome-dependent degradation was only reported as a mechanism of G2/M arrest in response to arsenite exposure (Chen *et al*, 2002).

Exposure to DNA damage activates p53 through ATM/ATR-dependent phosphorylation, which further inhibits cell-cycle progression through induction of CDK inhibitor p21 (Vousden and Prives, 2009). CHK2 checkpoint kinase also phosphorylates p53 leading to its stabilization and checkpoint activation (Chehab *et al*, 2000). In addition, the p53/p21 DNA damage response pathway plays a key role in monitoring telomere integrity at the G2/M transition during unchallenged

*Corresponding author. Telomere and Genome Stability Group, The CR-UK/MRC Gray Institute for Radiation Oncology and Biology, Department of Oncology, University of Oxford, Old Road Campus, Oxford OX3 7DQ, UK. Tel.: +44 01865 617319; Fax: +44 1865 617394; E-mail: madalena.tarsounas@oncology.ox.ac.uk
¹Present address: Department of Mechanistic Cell Biology, Max Plank Institute of Molecular Physiology, Dortmund, Germany

Received: 15 May 2012; accepted: 20 June 2012; published online: 27 July 2012

cell proliferation. Telomeres become transiently uncapped following their replication in S phase and the ensuing p53/p21 activation arrests cell-cycle progression to allow re-assembly of protective structures (Thanasoula *et al*, 2010). This mechanism prevents entry into mitosis when telomeres are exposed and resemble unrepaired DSBs.

Shelterin, a complex of six proteins (TRF1, TRF2, RAP1, TPP1, POT1 and TIN2) in mammalian cells, protects chromosome ends against degradation and fusion. The telomere-specific factor TRF2 acts together with TRF1 to anchor the shelterin complex onto the telomeric double-stranded DNA and plays a key role in telomere protection (Palm and de Lange, 2008). POT1, also a shelterin component, binds with sequence specificity to the single-stranded telomeric DNA and prevents deleterious checkpoint activation. In mouse embryonic fibroblasts (MEFs), telomeres artificially uncapped by conditional *Trf2* deletion elicit an ATM-dependent DNA damage response leading to non-homologous end-joining of dysfunctional telomeres (Celli and de Lange, 2005). In a similar system, *Pot1* gene inactivation triggered ATR-dependent signalling, which also promotes end-to-end fusions (Hockemeyer *et al*, 2006; Wu *et al*, 2006; Denchi and de Lange, 2007; Guo *et al*, 2007).

Here, we used human cells to demonstrate that during the G2/M transition TRF2- or POT1-depleted telomeres trigger either ATM/ATR-dependent p53 Ser15 phosphorylation or activation of CHK1/CHK2 checkpoint kinases. Both pathways converge to downregulate expression of CDC25C phosphatase, thus inhibiting CDK activity and preventing progression into mitosis in the presence of dysfunctional telomeres. Most unexpectedly, proteasome-mediated destruction of CDC25C is a key event in the response to uncapped telomeres, not required for the response to IR-induced DNA damage. CHK1/CHK2-dependent CDC25C phosphorylation at Ser216 destabilizes CDC25C by promoting its nuclear export and targeting it to the proteasome. This blocks mitotic entry in the presence of uncapped telomeres, thereby preventing end fusions deleterious for genome integrity.

Results

p53 prevents mitotic entry when telomeres become uncapped through loss of POT1 or TRF2

We have recently demonstrated that the p53/p21 pathway is required to prevent entry into mitosis when telomeres are artificially uncapped by inhibition of shelterin component TRF2 (Thanasoula *et al*, 2010). In human U2OS cells synchronized by double-thymidine block and release, TRF2 depletion triggered ATM/ATR-dependent phosphorylation of p53 at Ser15 and concomitant induction of p21, specifically at the G2/M transition. To address whether inactivation of other shelterin components in synchronized human cells triggers similar p53-dependent responses, we used siRNA-mediated depletion of POT1, a shelterin component which binds specifically to single-stranded telomeric DNA, thus suppressing ATR-dependent checkpoint responses (Palm and de Lange, 2008). Telomeres lacking POT1 elicited ATM/ATR-dependent p53 phosphorylation at Ser15 and an increase in p21 expression (Figure 1A), similarly to TRF2 inhibition. This response occurred in POT1-depleted cells between 9 and 11 h after double-thymidine block release when a significant proportion of cells were in G2/M as evaluated by FACS

analyses of DNA content (Supplementary Figure S1). This suggested that signalling pathways activated through TRF2 or POT1 inhibition converge to activate p53 and control mitotic entry.

TRF2 prevents ATM activation, while POT1 represses the ATR kinase (Palm and de Lange, 2008). To directly address whether p53 acts as an effector of both ATM- and ATR-dependent pathways in response to telomere damage, we monitored mitotic onset by measuring mitosis-specific phosphorylation of histone H3 at Ser 10 in cells lacking TRF2 or POT1. In human U2OS cells with an intact p53 pathway (Stott *et al*, 1998), we abrogated telomere capping by depleting either TRF2 or POT1, alone or in conjunction with p53 (Figure 1B). Inhibition of POT1 expression was monitored using real-time RT-PCR with *POT1*-specific primers, 24 h after siRNA treatment (Supplementary Figure S2A). Cell progression into mitosis was determined 10 h after release from a double-thymidine block, when cells were synchronized at the G2/M transition (Supplementary Figure S1). Inhibition of TRF2 or POT1 expression using siRNA significantly limited the ability to enter mitosis of U2OS cells with functional p53 (Figure 1C). Upon siRNA depletion of p53, both TRF2- and POT1-depleted cells entered mitosis at a slightly higher rate than GFP siRNA-treated control cells. This indicates that both types of telomere damage known to activate either ATM- or ATR-dependent responses, also triggered p53-dependent G2/M arrest. In the same cells, we quantified TIF formation by monitoring γ H2AX colocalization with the telomeric FISH signal (Figure 1D). The level of mitotic TIFs increased significantly upon co-depletion of p53 with either TRF2 or POT1 (Figure 1E), consistent with p53 playing a central role in the surveillance of telomere capping reactions at the G2/M transition. TIF quantification upon single POT1 or TRF2 depletion in U2OS cells proved not feasible due to the low numbers of metaphases generated. It was previously shown, however, that inactivation of shelterin components in p53-deficient mouse and human cells triggers high levels of mitotic TIFs (Martinez *et al*, 2009; Tejera *et al*, 2010; Thanasoula *et al*, 2010).

Uncapped telomeres trigger G2/M arrest through ATM/ATR-dependent p53 Ser15 phosphorylation

The mitotic entry block triggered by uncapped telomeres requires functional p53. We found that ATM/ATR-dependent p53 phosphorylation at Ser15 increased specifically during the G2/M transition. Thus, we tested whether inhibition of the ATM and ATR kinases could enable mitotic entry in cells with telomeres uncapped through loss of TRF2 or POT1, similarly to p53 inactivation. We treated POT1- or TRF2-depleted U2OS cells synchronized at the G2/M transition with the ATM inhibitor Ku55933 (Hickson *et al*, 2004) or ATR inhibitor ETP-46464 (Toledo *et al*, 2011; Figure 2A). POT1 depletion induced specifically Ser345 CHK1 phosphorylation, while TRF2 inactivation elicited robust CHK2 phosphorylation at Thr68 and weak CHK1 phosphorylation at Ser345. Depletion of TRF2 or POT1 led to p53 Ser15 and H2AX phosphorylation, which was diminished in the presence of ATM and ATR inhibitors. When used individually, each of the ATM and ATR inhibitors abolished phosphorylation of CHK1 in response to telomere damage, suggestive of a relatively low specificity of these inhibitors for the corre-

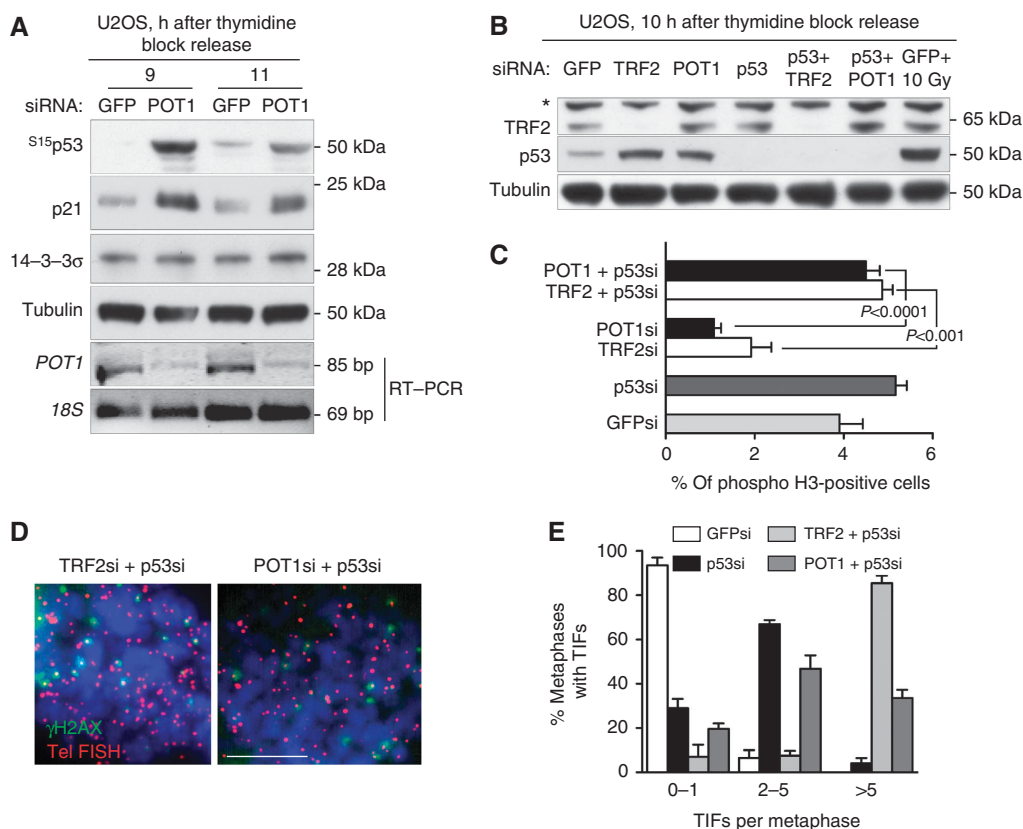


Figure 1 TRF2 and POT1 inhibition trigger a p53-dependent G2/M checkpoint response. **(A)** U2OS cells transfected with control GFP or POT1 siRNAs were grown for 48 h before synchronization by double-thymidine block and release. Cells collected at the indicated times after release were processed for immunoblotting or RT-PCR analysis as indicated. Tubulin and 18S were used as controls for western blotting and RT-PCR, respectively. **(B)** U2OS cells transfected with siRNA as shown were synchronized by double-thymidine block and release. After 10 h, extracts were prepared and immunoblotted as shown. Extracts from cells exposed to 10 Gy of IR were used as a control for p53 induction. *Non-specific band. **(C)** Cells treated as in **(B)** were stained with propidium iodide and an antibody against phosphorylated histone H3-Ser 10 and analysed by flow cytometry. $N = 10\,000$ cells were analysed for each sample. Error bars represent s.d. of at least two independent experiments. P -values were calculated using an unpaired two-tailed t -test. **(D)** Mitotic chromosomes isolated from U2OS cells treated with siRNA and arrested in mitosis with colcemid were spread onto glass slides using the cytopsin method. Preparations were fixed and stained with anti- γ H2AX monoclonal antibody (green). Telomeres were visualized with a Cy3-conjugated (CCCTAA)₆-PNA probe (red). Bar, 10 μ m. **(E)** Quantification of TIFs in U2OS cells treated as in **(D)**. A minimum of 100 metaphases were scored for each cell line. Error bars represent s.d. of two independent experiments. Figure source data can be found with the Supplementary data.

sponding kinases. Alternatively, chemical inhibition of ATM elicits ATR inactivation and loss of CHK1 phosphorylation, consistent with existing models of ATM and ATR acting sequentially in response to DSBs inflicted during S phase (Garcia-Muse and Boulton, 2005; Cuadrado *et al*, 2006; Jazayeri *et al*, 2006).

The G2/M arrest in TRF2 or POT1 siRNA-treated cells monitored with phospho-histone H3 staining was efficiently abrogated by treatment with Ku55933, ETP-46464 (Figure 2B) or caffeine (Supplementary Figure S2B and C), the latter known to compromise both ATM and ATR signalling. This suggests that both kinases are required to sustain the G2/M arrest in response to damaged telomeres. The low rate of mitotic entry following POT1 depletion was rescued by treatment with ATM inhibitor, reflecting activation of this kinase in POT1-deficient cells either directly through telomere uncapping or through accumulation of secondary intra-chromosomal DNA damage.

Both ATR and ATM kinases can phosphorylate p53 at Ser15 in response to DNA damage (Canman *et al*, 1998; Tibbetts *et al*, 1999). We detected the same phosphorylation event in response to telomere dysfunction triggered by loss of TRF2 or

POT1 during the G2/M transition (Thanasoula *et al*, 2010; Figure 1A). In addition, p53 can be phosphorylated at Ser20 by the CHK1 and CHK2 checkpoint kinases in response to DNA damage (Chehab *et al*, 2000; Hirao *et al*, 2000; Shieh *et al*, 2000). We therefore tested whether mutation of either of these two phosphorylation sites could alter the ability of p53 to mediate the G2/M arrest in response to dysfunctional telomeres. Human SAOS-2 cells lacking p53 function (Stott *et al*, 1998) were transfected with constructs expressing Ser15Ala and Ser20Ala substitutions of p53, following TRF2 or POT1 siRNA-mediated depletion. Exogenously expressed wild-type or mutant p53 were detected by western blotting in all cells, except for those transfected with vector only (Figure 2C). As expected, p53 Ser15 phosphorylation in response to TRF2 depletion was not detectable in cells expressing the Ser15Ala p53 mutant.

We next examined mitotic entry following telomere uncapping through TRF2 and POT1 inhibition. Progression into mitosis was impaired in p53-proficient cells (Figure 2D), suggestive of p53-dependent checkpoint activation. The Ser20Ala mutant p53 showed a low rate of mitotic entry similar to wild-type p53, which is consistent with the

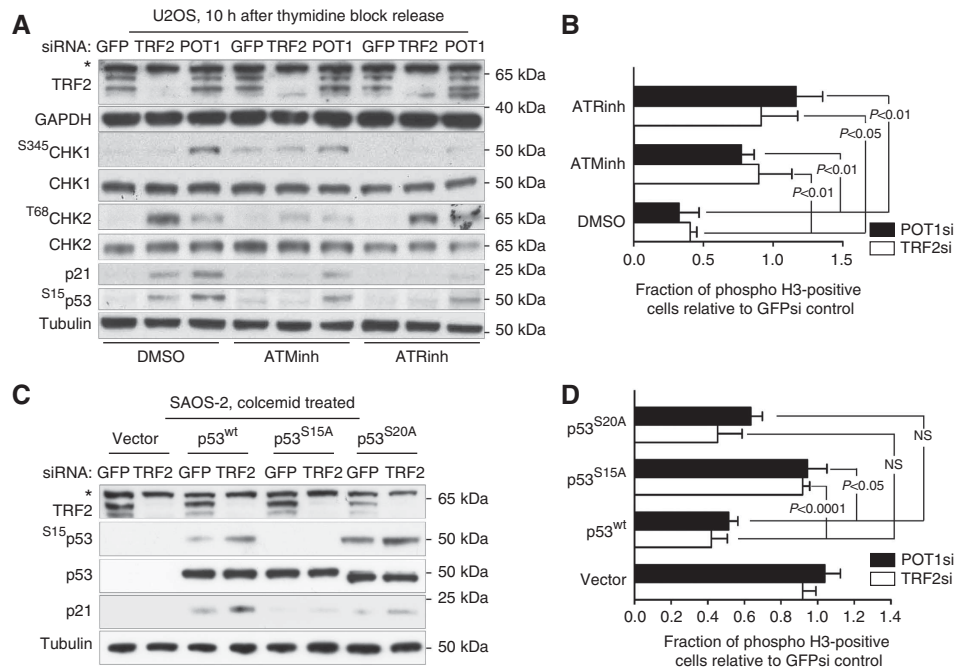


Figure 2 ATM/ATR-dependent phosphorylation of p33 at Ser15 prevents mitotic entry in response to telomeres uncapped by TRF2 or POT1 inhibition. **(A)** U2OS cells transfected with TRF2, POT1 or control GFP siRNAs were grown for 48 h before synchronization by double-thymidine block and release in fresh media for 10 h. ATM inhibitor (Ku55933), ATR inhibitor (ETP-46464) or solvent (DMSO) was added to media 4 h prior to collection. Cell extracts were prepared and immunoblotted as shown. *Non-specific band. **(B)** U2OS cells treated as in **(A)** were stained with propidium iodide and an antibody against phosphorylated histone H3-Ser 10 and analysed by flow cytometry. $N = 10\,000$ cells were analysed for each sample. Error bars represent s.d. of two independent experiments. P -values were calculated using an unpaired two-tailed t -test. **(C)** SAOS-2 cells were transfected with p53-encoding constructs or vector alone, 24 h after treatment with TRF2 or control GFP siRNAs. Cell extracts prepared 24 h later were immunoblotted as shown. Colcemid was added 3 h before collection. Tubulin was used as a loading control. *Non-specific band. **(D)** SAOS-2 cells treated as in **(C)** were stained with propidium iodide and an antibody against phosphorylated histone H3-Ser 10 and analysed by flow cytometry. $N = 10\,000$ cells were analysed for each sample. Error bars represent s.d. of at least two independent experiments. P -values were calculated using an unpaired two-tailed t -test. Figure source data can be found with the Supplementary data.

observed lack of p53 Ser20 phosphorylation in response to telomere dysfunction (Figure 4A). In contrast, cells expressing the Ser15Ala mutation, which abrogates ATM/ATR-dependent p53 phosphorylation, entered mitosis at a rate similar to that of control, vector-transfected, p53-deficient cells. Ser15Ala mutation also rescued mitotic entry in TRF2- and POT1-depleted WI38(VA13) human cells (Supplementary Figure S3A), known to lack a functional p53 pathway (Stott *et al*, 1998). These results demonstrate that ATM/ATR-dependent phosphorylation of p53 at Ser15, but not CHK1/CHK2-dependent Ser20 p53 phosphorylation is required for G2/M checkpoint activation in response to telomeres uncapped through TRF2 or POT1 inhibition.

CHK1 and CHK2 prevent mitotic entry with uncapped telomeres during physiological cell-cycle progression

We next addressed whether CHK1 and CHK2 checkpoint kinases, which are phosphorylated in response to artificially uncapped telomeres (Figure 2A), could also regulate telomere capping reactions prior to entry into mitosis. We thus inhibited CHK1 and CHK2 expression with siRNA in U2OS cells synchronized in G2/M (Figure 3A) and monitored the frequency of uncapped telomeres in mitosis using combined IF-FISH staining of mitotic chromosomes (Figure 3B). γ H2AX labelling of mitotic telomeres is rarely seen in U2OS cells, but it increases significantly upon p53 inhibition (Thanasoula *et al*, 2010). Similarly, we found that the number of γ H2AX-labelled telomeres in mitotic U2OS cells lacking CHK1 or

CHK2 is higher than in control cells (Figure 3C). This effect was however milder than the one caused by p53 abrogation, even when CHK1 and CHK2 are concomitantly depleted. In particular, CHK1-deficient cells show robust p53 Ser15 phosphorylation and p21 induction in G2/M (Figure 3A), suggesting that mitotic entry in these cells is primarily p53 dependent. We conclude that, in addition to p53, the checkpoint kinases CHK1 and CHK2 act to arrest proliferation and facilitate successful assembly of telomere capping structures before entry into mitosis.

CHK1 and CHK2 mediate the G2/M DNA damage response emanating from POT1- or TRF2-depleted telomeres

Conditional deletion of *Trf2* gene in MEFs triggers ATM-dependent CHK2 phosphorylation, while inactivation of *Pot1* induces ATR-dependent CHK1 phosphorylation (Denchi and de Lange, 2007). This led to the conclusion that TRF2 inhibits ATM and POT1 inhibits ATR-dependent signalling at mouse telomeres. Whether similar responses occur in human cells is unknown. Importantly, the assumption that human and mouse telomeres are structurally and functionally identical has been recently challenged with the discovery that mouse telomeres have two functionally distinct POT1 proteins, POT1a and POT1b. While combining features of both mouse proteins, human POT1 cannot compensate for the concomitant loss of *Pot1a* and *Pot1b* genes in mouse (Palm *et al*, 2009), suggesting a

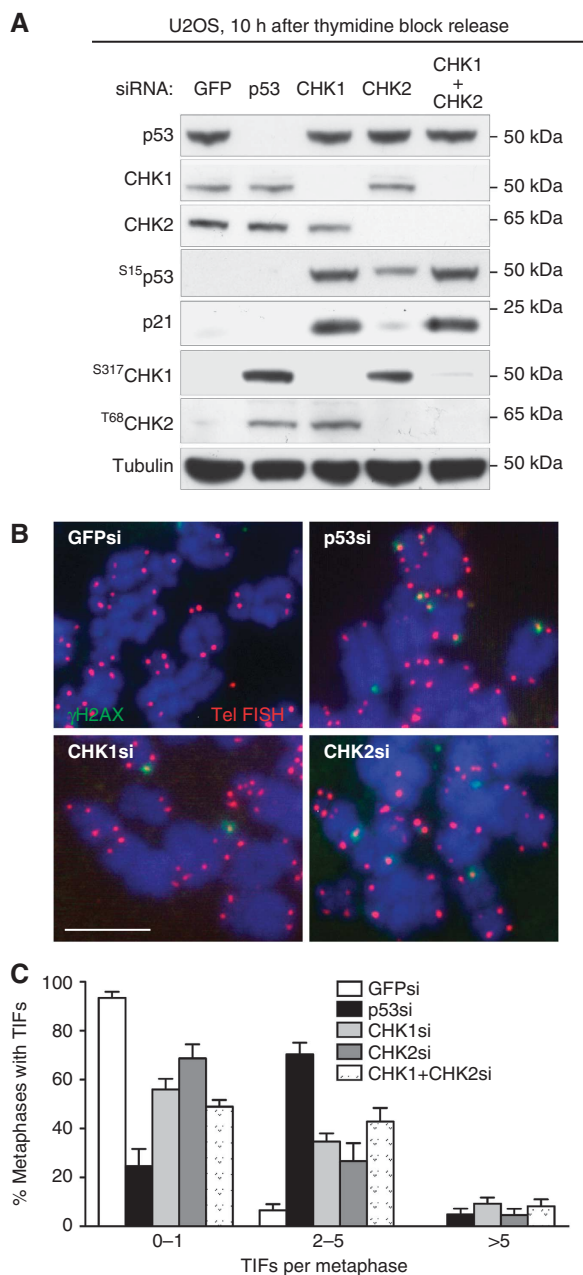


Figure 3 CHK1 and CHK2 act to monitor telomere integrity at the G2/M transition during physiologically normal cell-cycle progression. (A) U2OS cells were transfected with siRNA and grown for 48 h. Cell extracts were prepared and immunoblotted as indicated. (B) U2OS cells treated with p53, CHK1, CHK2 or GFP control siRNAs for 48 h were arrested in mitosis with colcemid and mitotic chromosomes were spread onto glass slides using the cytospin method. Preparations were stained with an anti- γ H2AX antibody (green) and a Cy3-conjugated (CCCTAA)₆-PNA probe (red). DNA was counter stained with DAPI (blue). Bar, 10 μ m. (C) TIF frequency was determined by counting the number of foci in 100–150 metaphases. Error bars represent s.d. of at least two independent experiments. Figure source data can be found with the Supplementary data.

clear evolutionary divergence in shelterin composition and function from rodent to human telomeres. Thus, we addressed whether the G2/M DNA damage response emanating from human telomeres uncapped through TRF2 or POT1 inhibition is similar to the one in mouse.

In human cells synchronized at the G2/M transition, we found that TRF2 depletion led to phosphorylation of CHK2 at

Thr68, while POT1 depletion induced CHK1 phosphorylation at Ser317 (Figure 4A). To directly address the ability of CHK1 and CHK2 to signal telomere damage and delay mitotic entry in the presence of artificially uncapped telomeres, we abrogated TRF2 and POT1 expression, alone, or in conjunction with CHK1 and CHK2 in human U2OS cells (Figure 4B). The ability to enter mitosis was measured through phosphohistone H3 immunostaining (Figure 4C), following double-thymidine block and release in fresh media for 10 h. Control GFP siRNA-treated U2OS cells exposed to 10 Gy of IR were efficiently arrested at the G2/M transition. While loss of TRF2 or POT1 expression in human U2OS cells impaired entry into mitosis, cell-cycle progression was restored efficiently by co-depletion of TRF2 together with CHK2, as well as of POT1 together with CHK1. Similar abrogation of the G2/M arrest was observed in POT1-depleted cells treated with CHK1 inhibitors UCN-01 and GÖ6976 (Supplementary Figure S3B). Treatment with these inhibitors led to an increase in CDC25A levels (Supplementary Figure S3C), as previously reported (Sorensen *et al*, 2003; Beck *et al*, 2010). To further explore the G2/M response to telomere uncapping, we measured TIF levels in TRF2- or POT1-depleted cells. TIFs occurred at high frequency in TRF2/CHK2 and POT1/CHK1 double-depleted mitotic cells (Figure 4D), reflecting abrogation of the G2/M checkpoint through CHK1 and CHK2 inhibition and progression into mitosis in the presence of damaged telomeres.

CHK1 and CHK2 promote G2/M arrest in response to uncapped telomeres through proteasome-mediated degradation of CDC25A and CDC25C phosphatases

During unchallenged cell proliferation, CDC25 phosphatases dephosphorylate CDK1(CDC2) and CDK2, which activates them and promotes G2/M transition. Upon exposure to DNA damaging agents, activated CHK1 and CHK2 phosphorylate and destabilize CDC25A and CDC25C to induce cell-cycle arrest (Bartek and Lukas, 2003). To address whether CHK1 and CHK2 could act similarly to prevent mitotic entry in response to uncapped telomeres, we monitored CDC25A and CDC25C levels in human cells synchronized at the G2/M transition. We detected both phosphatases in control cells transfected with GFP siRNA in G2/M (Figure 5A and B). Most unexpectedly, inhibition of TRF2 significantly reduced CDC25C levels, while CDC25A levels remained unchanged (Figure 5A). Consistent with the proliferation arrest in these cells being rescued by CHK2 inactivation (Figure 4C), we found that CDC25C levels were restored when CHK2, and to a lesser extent CHK1, was abrogated in TRF2-depleted cells. CDC25C was not downregulated by exposure to 10 Gy of IR, unlike CDC25A expression which was significantly reduced (Figure 5C; Supplementary Figure S3D), as previously reported (Sorensen *et al*, 2003; Melixetian *et al*, 2009). POT1 inhibition led to a decrease in CDC25A and CDC25C levels (Figure 5B), which were restored efficiently by concomitant treatment with CHK1 siRNA. Cyclin B expression decreased in both POT1 and TRF2-deficient cells, consistent with their impaired progression into mitosis. These results support the concept that telomere uncapping through TRF2 or POT1 inhibition triggers cell-cycle arrest through ATM/CHK2- or ATR/CHK1-dependent signalling, leading to degradation of CDC25A and CDC25C phosphatases.

TRF2 inhibition triggers global genomic instability through breakage-fusion bridge cycles. Therefore, the unexpected

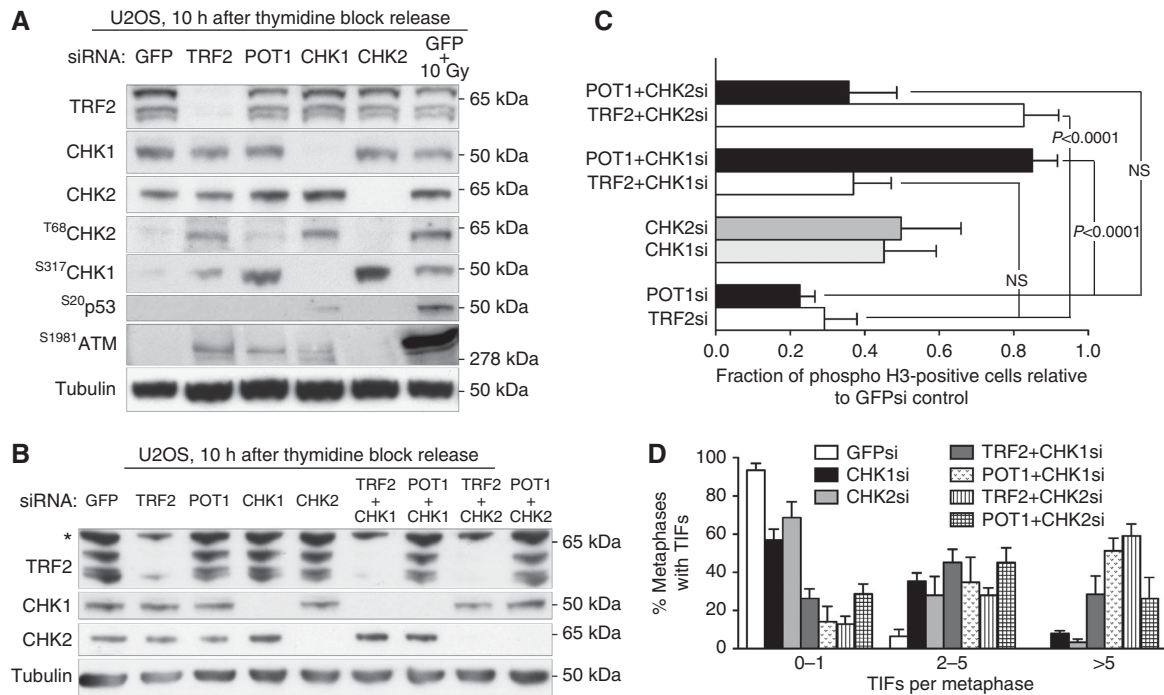


Figure 4 CHK1 and CHK2 mediate the G₂/M arrest elicited by artificially uncapped telomeres. **(A)** U2OS cells transfected with siRNA were grown for 48 h before synchronization by double-thymidine block and release. Cells collected 10 h after release were processed for immunoblotting as indicated. Extracts from cells exposed to 10 Gy of IR were used as a control for CHK1 and CHK2 phosphorylation. Tubulin was used as a loading control. **(B)** U2OS cells transfected with siRNA were grown for 48 h before synchronization by double-thymidine block and release. Cells collected 10 h after release were processed for immunoblotting as indicated. *Non-specific band. **(C)** U2OS cells treated as in **(B)** were stained with propidium iodide and an antibody against phosphorylated histone H3-Ser 10 and analysed by flow cytometry. *N* = 10 000 cells were analysed for each sample. Error bars represent s.d. of at least three independent experiments. *P*-values were calculated using an unpaired two-tailed *t*-test. **(D)** U2OS cells treated as in **(B)** were arrested in mitosis with colcemid and mitotic chromosomes were spread onto glass slides using the cytospin method. TIF frequency was determined by counting the number of γ H2AX foci colocalizing with telomeres in 100–150 metaphases. Error bars represent s.d. of at least two independent experiments. Figure source data can be found with the Supplementary data.

observation that CDC25A levels remain unaffected in TRF2-depleted cells raised the possibility that CDC25A stability is controlled by cell-cycle progression. To test this hypothesis, we synchronized TRF2-depleted U2OS cells in S and G₂/M stages of the cell cycle (Supplementary Figure S3D). While CDC25A levels were unaffected in G₂/M, cells in S phase showed a decrease in CDC25A expression in response to TRF2 depletion. CDC25C levels were decreased in S, while its expression was not detectable in G₂/M. CDC25A downregulation in response to IR was observed in both S and G₂/M, while CDC25C levels remained unchanged after IR exposure in both stages of the cell cycle. We therefore concluded that the response to TRF2-depleted telomeres is distinct from that triggered by intra-chromosomal breaks during the G₂/M transition in that it requires specifically CDC25C, but not CDC25A, destruction.

CDC25A and CDC25C degradation occurs through the ubiquitin-proteasome pathway (Chen *et al*, 2002; Melixetian *et al*, 2009). To test the possibility that this pathway becomes active upon telomere uncapping, we treated TRF2- and POT1-depleted U2OS cells synchronized at the G₂/M transition with the proteasome inhibitor MG132. This treatment led to stabilization of CDC25A and CDC25C, as well as of cyclin B in these cells (Figure 5C). Importantly, CDC2 Tyr15 phosphorylation was detected when CDC25C expression was abrogated by TRF2 or POT1 depletion, although CDC25A expression remained unchanged. This indicates that CDC2 is the main target of CDC25C during G₂/M transition in these cells.

Inhibiting protein degradation with MG132 reversed the mitotic entry block in cells with uncapped telomeres (Figure 5D). As a control, cells treated concomitantly with MG132 and colcemid did not show a different mitotic entry rate to those treated with MG132 alone, suggesting that under conditions used here mitotic progression does not occur at sufficiently high rates to justify additional mitosis trapping. In addition, telomerase-proficient HCT116 cells (Potts and Yu, 2007) showed CDC25C degradation (Supplementary Figure S4A) and G₂/M arrest (Supplementary Figure S4B) in response to telomere damage, both reversed by MG132 treatment. Similarly to the response in U2OS cells, IR-induced DNA damage did not alter CDC25C levels in HCT116 cells. Targeting TRF2 with esiRNA recapitulated the proteasome-mediated CDC25C destruction observed with TRF2 siRNA (Supplementary Figure S4C). Importantly, TRF2 and POT1 depletion led to CDC25C ubiquitylation detectable upon proteasome inhibition (Supplementary Figure S4D). This suggests that CDC25C undergoes ubiquitylation reactions in response to telomere damage, which targets it for proteasome-mediated degradation.

It is conceivable, however, that acute DNA damage inflicted through IR exposure triggers a response different from the one induced by chronic telomere uncapping. We therefore examined the response to chronic DNA damage caused by abrogation of homologous recombination activity of RAD51, which in human cells leads to G₂/M arrest, accumulation of unrepaired DSBs (data not shown) and ATM activation

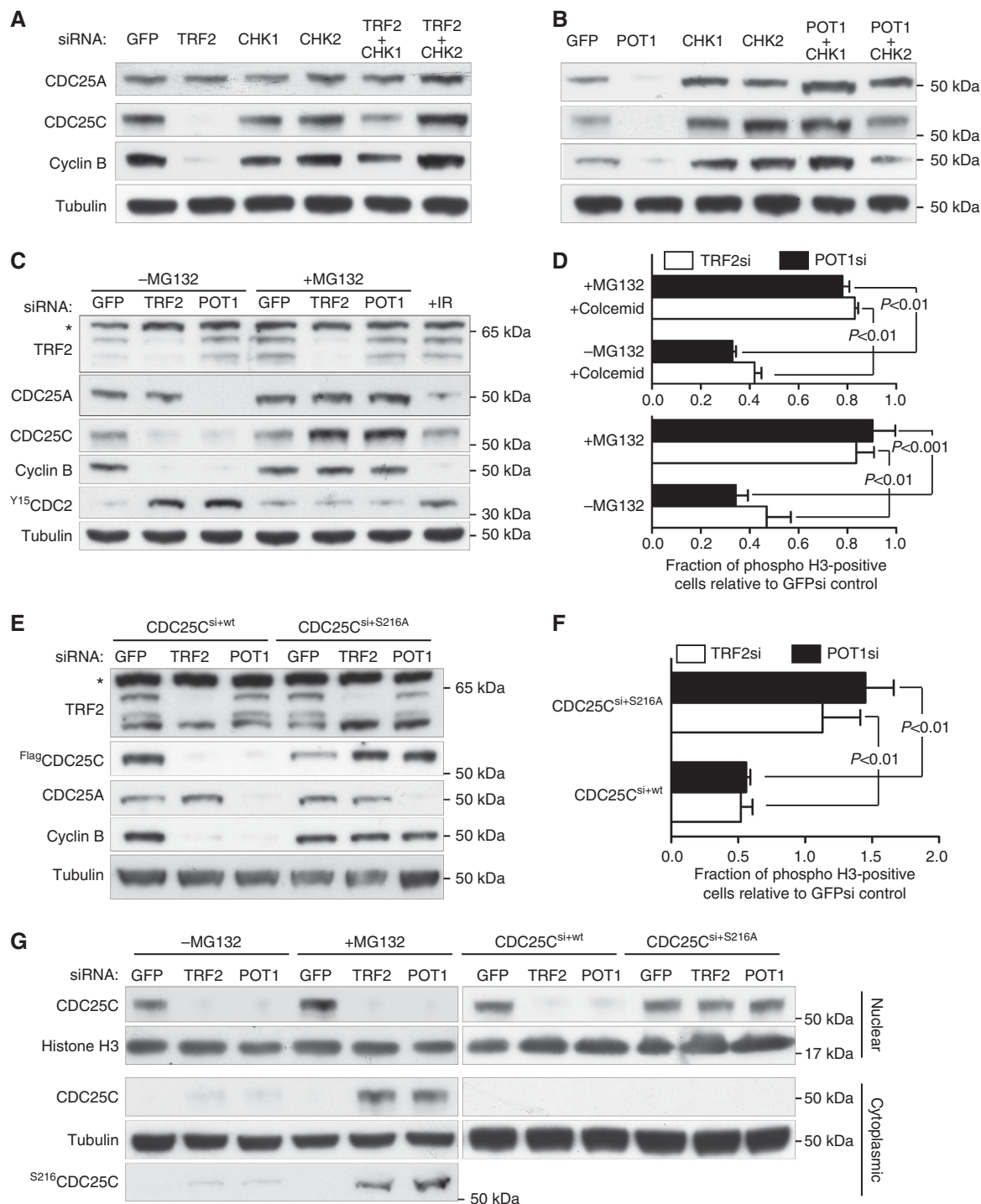


Figure 5 Proteasome-mediated destruction of CDC25C prevents mitotic entry in the presence of uncapped telomeres. **(A, B)** U2OS cells transfected with siRNA as shown were grown for 48 h before synchronization by double-thymidine block and release. Cells collected 10 h after release were processed for immunoblotting as indicated. Tubulin was used as a loading control. **(C)** U2OS cells transfected with TRF2, POT1 or control GFP siRNAs were grown for 48 h before synchronization by double-thymidine block and release in fresh media for 10 h. Proteasome inhibitor (MG132) was added to the media 3 h prior to collection. Cell extracts were prepared and immunoblotted as shown. Extracts from cells exposed to 10 Gy of IR were used as a control for CDC25A degradation. *Non-specific band. **(D)** U2OS cells treated as in **(C)** or treated with colcemid in addition to MG132, both added 3 h before collection, were stained with propidium iodide and an antibody against phosphorylated histone H3-Ser 10 and analysed by flow cytometry. $N = 10\,000$ cells were analysed for each sample. Error bars represent s.d. of three independent experiments. P -values were calculated using an unpaired two-tailed t -test. **(E)** U2OS cells were transfected with wild-type or S216A Flag-tagged CDC25C expression constructs in combination with CDC25C siRNA, 24 h after treatment with TRF2, POT1 or control GFP siRNAs. Twenty-four hours later, cells were synchronized in G2/M by double-thymidine block and release. Cell extracts prepared 10 h after release were immunoblotted as shown. *Non-specific band. **(F)** U2OS cells treated as in **(E)** were stained with propidium iodide and an antibody against phosphorylated histone H3-Ser 10 and analysed by flow cytometry. $N = 10\,000$ cells were analysed for each sample. Error bars represent s.d. of at least two independent experiments. P -values were calculated using an unpaired two-tailed t -test. **(G)** U2OS cells treated as in **(C)** or **(E)** were fractionated into nuclear and cytoplasmic extracts and immunoblotted as indicated. Figure source data can be found with the Supplementary data.

(Badie *et al*, 2009). Unlike TRF2 and POT1, RAD51 depletion from U2OS cells did not promote CDC25C destruction (Supplementary Figure S5A). Also contrary to the mitotic entry block induced by telomere damage, which is reversed by proteasome inhibition, failure to entry mitosis of cells depleted of RAD51 or treated with IR was not rescued by the MG132 treatment (Supplementary Figure S5B). The IR-mediated G2/M arrest was also unaffected by inhibition of protein degradation. We thus concluded that proteasome-mediated degradation of CDC25C is a G2/M response specific to telomere damage and distinct from that triggered by acute IR-induced DNA damage or by chronic DSBs accumulation following abrogation of recombinational repair.

Two distinct pathways downregulate CDC25C in response to telomere dysfunction to prevent progression into mitosis

CDC25C phosphorylation at Ser216 is critical for CDC2 inactivation and timing of cell-cycle transitions (Takizawa and Morgan, 2000). We thus addressed whether this residue is also important for the cellular responses to damaged telomeres. In TRF2- or POT1-depleted U2OS cells, we inhibited CDC25C expression using siRNA and ectopically expressed siRNA-resistant, FLAG-tagged wild-type CDC25C or the Ser216Ala CDC25C mutant (Figure 5E; Bulavin *et al*, 2003). Ectopically expressed wild-type CDC25C was degraded in response to TRF2 and POT1 inhibition, while Ser216Ala mutant levels did not change. This suggests that Ser216 phosphorylation targets CDC25C for proteasome-mediated degradation. Moreover, the mitotic entry block elicited by TRF2 or POT1 inhibition was maintained in cells in which wild-type CDC25C expression was ectopically restored following siRNA-mediated depletion of endogenous CDC25C (Figure 5F). The fraction of cells progressing into mitosis was significantly enhanced by expression of the Ser216Ala CDC25C mutant. Thus, CDC25C is an important downstream target of the CHK2-dependent checkpoint activated by uncapped telomeres at the G2/M transition.

G2/M checkpoint activation by DNA damage requires exclusion of CDC25C from the nucleus, achieved through 14-3-3 binding of Ser216-phosphorylated CDC25C (Peng *et al*, 1997). To examine the intracellular distribution of CDC25C in response to telomere damage, we performed fractionation of G2/M cellular extracts depleted of TRF2 or POT1, in the presence or absence of proteasome inhibitor (Figure 5G). In control GFP siRNA-treated cells, CDC25C is present in the nucleus and is degraded in response to TRF2 or POT1 depletion. Upon inhibition of protein degradation, stabilized CDC25C re-localizes to the cytoplasm, which suggests that nuclear export is required for its proteasomal destruction. Under these conditions, we detect Ser216-phosphorylated CDC25C in the cytoplasm, supporting the concept that cytoplasmic Ser216-phosphorylated CDC25C is targeted for destruction. Importantly, abrogation of CDC25C Ser216 phosphorylation leads to CDC25C accumulation in the nucleus. Thus, checkpoint-dependent Ser216 phosphorylation promotes CDC25C export into the cytoplasm, where it is targeted for proteasome degradation.

Expression of the Ser216Ala CDC25C mutant caused a significant increase in the fraction of cells progressing into mitosis (Figure 5F), to levels even higher than CHK1 and CHK2 abrogation (Figure 4C) or p53 deficiency (Figure 2D).

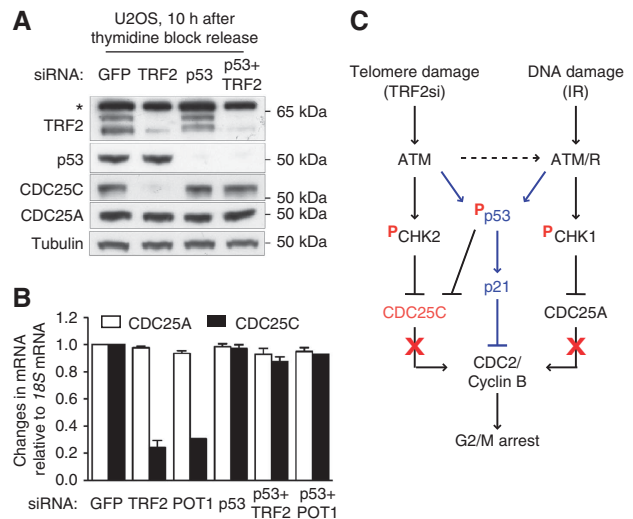


Figure 6 Telomeres uncapped through TRF2 or POT1 depletion trigger p53-dependent transcriptional downregulation of CDC25C. (A) U2OS cells transfected with siRNAs as shown were grown for 48 h before synchronization by double-thymidine block and release. Cells collected 10 h after release were processed for immunoblotting as indicated. Tubulin was used as a loading control. *Non-specific band. (B) mRNA was isolated from U2OS cells treated as in (A). The levels of CDC25A and CDC25C transcripts were determined by real-time RT-PCR. (C) Comparison between the G2/M canonical DNA damage response and the response elicited by telomeres uncapped through TRF2 depletion. Both types of damage trigger ATM/ATR signalling leading to p53 activation and p21 upregulation, known to inhibit CDK activity and entry into mitosis. Telomere uncapping through TRF2 depletion activates ATM signalling, which leads to CHK2-dependent CDC25C degradation and cell-cycle arrest. In addition, p53 downregulates CDC25C at transcriptional level in response to telomere dysfunction. DNA damage induced by IR exposure elicits ATM/ATR activation, which in G2/M leads to CHK1-dependent CDC25A destruction and cell-cycle arrest. Figure source data can be found with the Supplementary data.

This suggests that mechanisms additional to CHK1/CHK2 phosphorylation regulate CDC25C turnover. Human *CDC25C* gene was identified as a target for transcriptional repression by p53 (St Clair *et al*, 2004), raising the possibility that a similar p53-dependent mechanism contributes to CDC25C downregulation in response to uncapped telomeres. To test this hypothesis, we determined CDC25C mRNA levels using real-time RT-PCR in p53-proficient and p53-deficient cells, in which TRF2 was depleted using siRNA (Figure 6A). The decrease in *CDC25C* mRNA levels observed upon TRF2 inhibition in cells with intact p53 was abolished in p53-deficient cells (Figure 6B). Consistent with this, CDC25C protein levels were partially restored when TRF2 and p53 were concomitantly depleted (Figure 6A). CDC25A protein and mRNA levels remained unchanged in response to TRF2 depletion. These results suggest that CDC25C downregulation, a key event in the G2/M checkpoint response to uncapped telomeres, is controlled through two distinct pathways: proteasome-mediated degradation and p53-dependent transcriptional repression.

Discussion

Ensuring genomic integrity before cells have committed to mitosis is essential for the accurate transmission of genetic material to offspring and to sustain cell proliferation. The

G2/M checkpoint plays a critical role in preventing cells from entering mitosis and segregating their chromosome in the presence of DNA damage. In addition to spontaneous breaks that arise during DNA replication, uncapped telomeres provide an intrinsic source of DNA damage that can trigger G2/M checkpoint activation. Telomeres become transiently uncapped in every cell cycle, following their replication and elongation during S phase. Reconstitution of telomere protective structures is a stochastic process and a G2/M delay is required to allow recapping of all chromosome ends. We have previously shown that the p53/p21 pathway is required during physiological G2/M transition to delay mitotic entry until telomere protective structures are re-assembled at all chromosome ends (Thanasoula *et al*, 2010). Cells lacking p53 activity progress into mitosis with uncapped telomeres, which are sensed as DNA damage and become rejoined in G1, which could initiate recurring cycles of chromosome instability (Maser and DePinho, 2002).

p53/p21 and CHK1/CHK2 provide separate pathways to monitor telomere integrity during the G2/M transition

In spite of its importance for genome integrity, little is known about the mechanism of G2/M checkpoint activation by uncapped telomeres. Here, we provide evidence that telomere uncapping through depletion of TRF2 or POT1, two key components of the shelterin complex, blocks progression into mitosis through ATM/ATR-dependent phosphorylation of p53, CHK1 and CHK2. These, in turn, prevent activation of the CDC2/cyclin B complex through enhanced transcription of cyclin-dependent kinase inhibitor p21 or downregulation of CDC25 phosphatases (Figure 6C).

p53 is a key player in the G2/M DNA damage response emanating from uncapped telomeres (Thanasoula *et al*, 2010). The results presented here demonstrate that p53 Ser15, known to undergo ATM/ATR-dependent phosphorylation in response to intra-chromosomal DSBs (Canman *et al*, 1998; Tibbetts *et al*, 1999), is also essential to prevent mitotic entry of cells with telomeres damaged through TRF2 or POT1 depletion. An important implication of these results is that the G2/M response to uncapped telomeres requires ATM and ATR activity. Indeed, chemical inhibition of either of the two phosphoinositide 3 kinases leads to abrogation of the G2/M arrest and premature entry into mitosis in the presence of telomere damage, which ultimately triggers telomere-induced genomic instability.

In this study, we extended the molecular targets of the G2/M checkpoint activated by damaged telomeres to show that CHK1 and CHK2 checkpoint kinases play key roles in preventing mitotic entry in response to uncapped telomeres. CHK1 and CHK2 are differentially activated during G2/M by distinct types of telomere damage. POT1-depleted telomeres elicit an ATR-dependent response and downstream CHK1 phosphorylation, most likely through exposure and excessive production of the G-rich single-stranded telomeric DNA (Hockemeyer *et al*, 2006; Wu *et al*, 2006). Surprisingly, we also detected ATM activation through Ser1981 phosphorylation in response to POT1 depletion, which could be the result of secondary intra-chromosomal DNA damage caused by telomere uncapping, as previously reported in mouse models (Hockemeyer *et al*, 2006). Alternatively, exposed single-stranded telomeric DNA could trigger ATM activation, as

previously reported for uncapped telomeres that cannot be rejoined in *Trf2*^{-/-} *LigIV*^{-/-} MEFs (Celli and de Lange, 2005).

We showed that in human cells TRF2 depletion activates ATM and triggers phosphorylation of its specific target, CHK2, similarly to *Trf2* deletion in MEFs. In addition, we detected CHK1 phosphorylation, indicative of ATR activation, in TRF2-depleted cells, which reflects ATM-dependent activation of ATR by damaged telomeres, similarly to the response to IR-induced DSBs (García-Muse and Boulton, 2005; Cuadrado *et al*, 2006; Jazayeri *et al*, 2006). The similarity to the canonical DNA damage response is extended by our observation that CHK1 phosphorylation at Ser317 in response to POT1 depletion was efficiently abolished by ATM inhibition, as previously reported for the IR response (Gatei *et al*, 2003). Moreover, CHK1 phosphorylation was enhanced in G2/M cells lacking CHK2 and conversely, CHK2 phosphorylation was detectable in cells lacking CHK1, suggestive of compensatory effect and cross-talk between the ATM and ATR-dependent checkpoint response pathways (Bartek and Lukas, 2003).

Mitotic entry is restored in cells lacking POT1 or TRF2 through CHK1 or CHK2 inhibition, respectively. Importantly, this occurs in U2OS cells with functional p53, suggesting that CHK1 and CHK2 act in a pathway independent of p53 in the G2/M response elicited by damaged telomeres. Importantly, our data indicate that CHK1 or CHK2 abrogation is less effective than p53 inhibition in suppressing the G2/M arrest triggered by uncapped telomeres. The average fraction of cells entering mitosis following TRF2 and p53 co-depletion relative to control GFP siRNA-treated cells was 1.19, while only 0.83 of the TRF2- and CHK2-deficient cells entered mitosis. The corresponding average mitotic fractions for POT1 co-depletion with p53 or CHK1 were 1.09 and 0.85, respectively. Thus, p53 is a more potent mediator of the G2/M arrest in response to uncapped telomeres than either of the two checkpoint kinases. This is most likely because p53 acts to repress CDK through two distinct mechanisms, p21 induction and transcriptional CDC25C downregulation, which enhance the p53 effect on mitotic entry.

p53 and CHK1/CHK2 provide independent pathways to monitor telomere capping reactions during physiologically normal cell-cycle progression. Here, too, p53 is a more potent checkpoint mediator, possibly because it requires a lower threshold of telomere damage to become activated, compared to the CHK1- or CHK2-dependent response. This is reflected in the higher level of mitotic TIFs in p53-deficient cells, compared to cells lacking CHK1 or CHK2. Alternatively, spontaneous replication-associated telomere damage in cells lacking p53, in addition to incomplete post-replicative telomere capping, could account for the elevated TIF levels.

CDC25C downregulation promotes G2/M arrest in response to uncapped telomeres

Inhibiting expression of TRF2 or POT1 shelterin components generates telomere structural aberrations, which activate distinct chromosome integrity surveillance pathways. Here, we show that these pathways converge to lower the mitosis-promoting activity of CDC2/cyclin B kinase and block mitotic entry. Degradation and/or inhibition of CDC25 phosphatase family members through CHK1 or CHK2 activation elicit cell-

cycle arrest after exposure to DNA damaging agents (Bartek and Lukas, 2003; Kastan and Bartek, 2004). Our results suggest that regulation of CDC25 stability in response to uncapped telomeres depends on the type of telomere damage: POT1 depletion led to a decrease in both CDC25A and CDC25C levels, while TRF2 abrogation promoted only CDC25C destruction. Both effects are abolished by CHK1 or CHK2 inactivation, respectively, as well as by proteasome inhibition. This is in contrast to the G2/M response to IR-induced DSBs, in which CHK1-dependent destruction of CDC25A is sufficient to arrest cell-cycle progression (Falck *et al*, 2001; Sorensen *et al*, 2003; Melixetian *et al*, 2009). Interestingly, both CDC25A and CDC25C expression levels were reduced in TRF2-depleted cells in S phase (Supplementary Figure S3D), suggesting that distinct checkpoints are activated by telomere damage in S and G2/M. CDC25C expression was not affected by IR exposure in either S or G2/M (Figure 5C; Supplementary Figure S3D; Xiao *et al*, 2003). Thus, the response to uncapped telomeres during G2/M transition is clearly different from that elicited by unrepaired DSBs in that the former requires proteasome-dependent destruction of the cell-cycle regulator CDC25C.

One possible explanation for this intriguing result is that telomere damage signalling in G2/M is primarily channelled through CHK2, which controls CDC25C stability. While this hypothesis has not yet been experimentally validated, it was established that acute IR-induced damage is channelled through CHK1, which targets CDC25A for degradation. Consistent with this, CHK1 is essential for IR-dependent CDC25A turnover, while CHK2 is not generally required for this response (Jin *et al*, 2008). Conversely, CHK2 may play a more important role than CHK1 in regulating CDC25C stability in response to telomere damage during G2/M transition. Supporting this concept is the robust CHK2 phosphorylation triggered by TRF2-depleted telomeres. This possibly reflects ATM activation caused by attrition of the 3' telomere overhang (Shiotani and Zou, 2009), a well-established consequence of TRF2 deficiency (Celli and de Lange, 2005). Nevertheless, our results do not exclude the possibility that CDC25A degradation contributes to the early response to uncapped telomeres. To ascertain this, a robust experimental system to rapidly deplete TRF2 is required, which will enable accurate monitoring of CDC25A and CDC25C stability at early and late time points following induction of telomere damage.

Importantly, CDC25C Ser216 can be phosphorylated by CHK2 *in vitro* (Matsuoka *et al*, 1998) and we show that it promotes CDC25C cytoplasmic re-localization, ubiquitylation and proteasome degradation in response to uncapped telomeres. Ser216Ala mutant abrogates CDC25C cytoplasmic translocation and effectively restores mitotic entry in cells with uncapped telomeres. Moreover, CDC25C expression in response to TRF2 depletion is regulated at transcriptional level in p53-dependent manner. This supports the notion that telomere damage-activated G2/M checkpoint promotes CDC25C downregulation through at least two pathways. The contribution of CDC25A degradation to the G2/M arrest induced by POT1 depletion provides an additional layer of complexity to the mechanism of checkpoint activation by dysfunctional telomeres. As CDC25A and CDC25C can dephosphorylate and activate both CDK1 and CDK2, it is

conceivable that multiple pathways regulate mitotic entry and their interplay is far more complex than previously appreciated. How these pathways interact and compete with each other to adjust the G2/M response to signals emanating from dysfunctional telomeres or other types of DNA damage remains to be determined.

Materials and methods

Cell lines, culture conditions and treatments

U2OS, SAOS-2, WI38-VA13 and p53-proficient HCT116 (all obtained from Cancer Research UK Cell Services) were cultivated in monolayers in DMEM medium (Invitrogen) supplemented with antibiotics (penicillin and streptomycin; Sigma-Aldrich) and 10% fetal bovine serum (FBS, Invitrogen). γ -Irradiation was carried out using a ^{137}Cs source at the dose indicated. Human cells were arrested in mitosis by addition of 0.1 $\mu\text{g}/\text{ml}$ colcemid (Gibco) to the media, followed by 7–12 h incubation at 37°C. ATM inhibitor Ku-55933 (R&D Chemicals; 10 μM), caffeine (Sigma-Aldrich; 5 mM), ATR inhibitor ETP-46464 (a gift from Dr Oscar Fernandez Capetillo; 5 μM), UCN-01 (Merck-Chemicals; 300 nM) and Gö6976 (Tocris Bioscience; 300 nM) were added to the media 4 h prior to collection of cells released from a double-thymidine block. MG132 (Calbiochem; 5 μM) was added to the media 3 h prior to collection of cells released from a double-thymidine block.

siRNA

U2OS cells were transfected using DharmaFect (Thermo Scientific). Briefly, $1.5\text{--}2 \times 10^6$ cells were reverse transfected in 10 cm plates, using 40 nM siRNA/plate and processed 48 h later. siRNA duplexes were 21 base pairs with 2-base deoxynucleotide overhang (Dharmacon Research). A GFP siRNA with the sequence GCTGACC CTGAAGTTCATCTT was used as a control. The sequence of human p53 siRNA was GCAUCUUAUCCGAGUGGAAUU (Thanasoula *et al*, 2010), of TRF2 siRNA CAGAAGUGGACUGUAGAAGUU (Takai *et al*, 2003), POT1 siRNA CAGGAGUACUAGAAGCCUA (siGENOME no. 18), CHK1 siRNAs were CAAGAUUGUGGUACUUUA and CCACAU GUCCUGAUCUAU (ON-TARGETplus, no. 10 and no. 12), CHK2 siRNAs (siGenome SMARTpool) were CUCAGGAACUCUAUUCUAU, AAACGCCGUCCUUUGAAUA, GCUAAAUCAUCCUUGCAUC, GAAA UUGCACUGUCACUAA and CDC25C siRNA against 5' untranslated region was GCCUUGAGUUGCAUAGAGAUU. The TRF2 esiRNA was from Mission esiRNA (HU-08111; Sigma). Two days after siRNA transfection, U2OS cells were either harvested by trypsinization and processed for immunoblotting, or treated with 0.1 mg/ml colcemid (Gibco), then harvested by trypsinization and processed for combined immunofluorescence (IF)-FISH, or treated with 2 mM thymidine for the cell synchronization protocol.

SAOS-2 and WI38-VA13 human cells were first treated with siRNA as above, then transfected 24 h later with p53-encoding DNA constructs (gift from Dr Xuan Liu, University of California; Shouse *et al*, 2008) using Lipofectamine (Invitrogen). Cells were collected 24 h after transfection and processed for western blotting, anti-phosphorylated histone H3-Ser 10 staining and FACS analysis.

Real-time RT-PCR

To determine *POT1* mRNA levels following siRNA-mediated depletion, real-time RT-PCR using the Fast SYBR[®] Green Cells-to-CT™ kit (Applied Biosystems) was performed 24 h after siRNA transfection. The primers used to amplify *POT1* mRNA were TCAGATGTTATCTG TCAATCAGAACCT and TGTTGACATCTTCTACCTCGTATAATGA and to amplify *18S*: AGTCCCTGCCCTTTGTACACA and GATCCGAG GGCTCACTAAAC. Real-time RT-PCR was also used to determine *CDC25A* and *CDC25C* mRNA levels in G2/M following siRNA-mediated depletion of TRF2 and POT1. The primers used to amplify *CDC25A* mRNA were GCCTGTCCACCAACCTGAC and CCAGGAGAA TCTAGACAGAAACC (Sarkar *et al*, 2010) and to amplify *CDC25C*: GAACAGGCCAAGACTGAAGC and GCCCTGGTTAGAATCTTCC (Le Gac *et al*, 2006).

Synchronization of human cells

Synchronization of U2OS cells was performed using a double-thymidine block. Briefly, exponentially growing cells were arrested

by addition of thymidine (Sigma-Aldrich; 2 mM final concentration) to the media for 16 h, followed by two washes in PBS and release into fresh media for 10 h. Cells were then arrested a second time by addition of thymidine (2 mM) and 16 h incubation, then washed as above and released into fresh media. Samples were collected at the indicated time points for western blotting, anti-phosphorylated histone H3-Ser 10 staining and FACS analysis.

FACS analysis

Cells were harvested by trypsinization, washed in cold PBS and fixed in ice-cold 70% ethanol overnight at -20°C . Following one wash in PBS, cells were incubated with 5 $\mu\text{g}/\text{ml}$ propidium iodide and 0.25 mg/ml RNase I (Sigma-Aldrich) in PBS. At least 10 000 cells were analysed by flow cytometry (Becton Dickinson). Data were processed using CellQuest (Becton Dickinson).

Anti-phosphorylated histone H3 staining

Cells were harvested by trypsinization, washed once in cold PBS and fixed in 1% paraformaldehyde in PBS (pH 7.5–8) at 37°C for 10 min. Following permeabilization in ice-cold 90% methanol, cells were washed in PBS twice and blocked in FACS incubation buffer (0.5% BSA in PBS) for 45 min at room temperature. Cells were stained with anti-phosphorylated histone H3-Ser 10 (Cell Signalling) antibody diluted 1:50 in FACS incubation buffer and FITC-conjugated anti-mouse IgG antibody (Jackson ImmunoResearch) diluted 1:100 in FACS incubation buffer. Following one wash in PBS, cells were incubated with 5 $\mu\text{g}/\text{ml}$ propidium iodide and 0.25 mg/ml RNase I (Sigma-Aldrich) in PBS. At least 10 000 cells were analysed by flow cytometry (Becton Dickinson). The rate of mitotic entry of cells transfected with control GFP siRNA (Supplementary Figure S5C) was similar between experiments. To facilitate comparison, we reported most of the results as fraction of phosphorylated histone H3-positive cells in samples treated with various siRNAs normalized to phosphorylated histone H3-positive cells in the GFP siRNA control cells, instead of absolute percentages of phosphorylated histone H3-positive cells in individual cell populations.

Cell fractionation

Cells were harvested by trypsinization, washed in cold PBS and resuspended in cold buffer A + (10 mM HEPES pH 7.9, 10 mM KCl, 1.5 mM MgCl_2 , 0.34 M sucrose, 10% glycerol and protease inhibitors; Mendez and Stillman, 2000) at a concentration of 2×10^7 cells/ml. Following 5 min incubation on ice, the extract was centrifuged for 5 min at 1300 g. The supernatant was collected and cleared by centrifugation at 20 000 g for 20 min to generate the cytoplasmic fraction of the cell extract. The pellet obtained after the 1300 g centrifugation was washed in buffer A +, resuspended in SDS-PAGE loading buffer at a concentration of 5×10^7 cells/ml and sonicated to generate the nuclear fraction of the cell extract.

Immunoprecipitation

Cells were harvested by trypsinization, washed in cold PBS, resuspended in cold lysis buffer (50 mM Tris pH 8.0, 0.5 M NaCl, 0.4% NP-40, 10% glycerol, 1 mM DTT, 1 mM PMSF and protease inhibitors; Roche), incubated on ice for 15–30 min and sonicated. Extracts were then centrifuged at 18 000 g for 20 min at 4°C and the supernatants were stored at -20°C . For immunoprecipitation, supernatants were diluted 1:3 in dilution buffer (50 mM Tris pH 8.0, 0.4% NP-40, 10% glycerol, 1 mM DTT, 1 mM PMSF and protease inhibitors; Roche) and incubated with Protein A-Dynabeads (Invitrogen) crosslinked with IgG or anti-CDC25C antibody (C-20; Santa Cruz) at 4°C for 2 h with rotation. Following three washes in lysis buffer, the pellet was resuspended in sample buffer. Eluted proteins were analysed by gel electrophoresis and western blotting.

Immunoblotting

Cells were harvested by trypsinization, washed with cold PBS, resuspended in SDS-PAGE loading buffer at a concentration of 2×10^7 cells/ml and sonicated. Equal amounts of protein (50–100 μg) were analysed by gel electrophoresis followed by western blotting. NuPAGE-Novex 10% Bis-Tris and NuPAGE-Novex 3–8% Tris-Acetate gels (Invitrogen) were run according to manufacturer's instructions. Anti- α -tubulin antibody was used as loading control. To detect phosphorylated and non-phosphorylated forms of the

same protein, two gels loaded with equal amounts of protein from the same samples were run in parallel and immunoblotted with the corresponding antibodies. Equal loading was established for each gel using antibodies against tubulin.

IF-FISH

For IF-FISH staining, metaphase spreads were fixed in 4% paraformaldehyde with 0.1–0.5% Triton X-100 in PBS, permeabilized with 0.5% Triton X-100 in PBS and subjected to IF staining as described (Tarsounas *et al*, 2004). Briefly, metaphase spreads were incubated in antibody dilution buffer (1% goat-serum, 0.3% BSA, 0.005% Triton X-100 in PBS) for 10 min, then in primary antibody overnight. Following three washes in antibody dilution buffer supplemented with 0.005% Triton X-100, Alexa 433-conjugated secondary antibody was added for 1 h. All antibody incubations were at room temperature. Samples were then washed and fixed again in 4% paraformaldehyde in PBS. Following three washes in PBS, slides were briefly dried at room temperature. FISH was performed as described (Tarsounas *et al*, 2004) using 15 $\mu\text{g}/\text{ml}$ Cy3-conjugated [CCCTAA]₆-PNA telomeric probe (Applied Biosystems). Chromosomes were visualized with DAPI. Slides were mounted using ProLong Antifade (Invitrogen) supplemented with 1 mg/ml 4,6-diamidino-2-phenylindole (DAPI). Specimens were viewed at room temperature with a Leica DMI6000B inverted microscope and fluorescence imaging workstation equipped with a HCX PL APO $\times 100/1.4$ –0.7 oil objective, and images acquired using a Leica DFC350 FX R2 digital camera using LAS-AF software (Leica). Brightness levels and contrast adjustments were applied to the whole image using Photoshop CS3 (Adobe).

Antibodies

The following antibodies were used for immunoblotting: rabbit polyclonal antisera raised against human TRF2 (Tarsounas *et al*, 2004), phospho-p53 Ser15 (Cell Signalling), phospho-p53 Ser20 (Cell Signalling), p21 (C-19, Santa Cruz Biotechnology), CDC25C (C-20, Santa Cruz), CHK1 (Cell Signalling), human phospho-CHK1 Ser317 (Cell Signalling), human phospho-CHK2 Thr68 (Cell Signalling), phospho-CDC25C Ser216 (Cell Signalling) and human histone H3 (a gift from Dr Alain Verreault, University of Montreal); goat polyclonal antibody raised against phospho-CDC2 Tyr15 (sc-7989; Santa Cruz); mouse monoclonal antibodies raised against mouse TRF1 (TRF-78; Abcam), p53 (DO-1; Santa Cruz Biotechnology), 14-3-3 σ (Upstate), CHK2 (Clone 7; Millipore), CDC25A (F-6; Santa Cruz Biotechnology), phospho-ATM Ser1981 (Cell Signalling), c-myc (9E10; Millipore) and α -tubulin (Cancer Research UK Monoclonal Antibody Service). In addition, a mouse monoclonal antibody raised against phosphorylated histone H2AX-Ser139 (JBW301; Upstate) was used for IF detection.

Supplementary data

Supplementary data are available at *The EMBO Journal* Online (<http://www.embojournal.org>).

Acknowledgements

We thank Dr Xuan Liu (University of California, Riverside, USA) for kindly supplying the p53 wild-type and mutant constructs, Dr Oskar Fernandez-Capetillo (CNIO, Madrid) for the gift of ATR inhibitor, Dr DV Bulavin (National University of Singapore) for the CDC25C wild-type and mutant expression vectors and M Woodcock for assistance with FACS analysis. We would also like to thank Wade Harper for insightful comments on this work. Research in MT's laboratory is supported by Cancer Research UK, EMBO Young Investigator Programme and The Royal Society.

Author contributions: M Tarsounas conceived the original idea and wrote the manuscript. M Tarsounas and M Thanasoula designed and planned the experiments. M Thanasoula executed most of the experiments. JE processed samples for FACS analysis. JE and NS performed the experiment in Figure 2A.

Conflict of interest

The authors declare that they have no conflict of interest.

References

- Ahn J, Urist M, Prives C (2004) The Chk2 protein kinase. *DNA Repair* **3**: 1039–1047
- Badie S, Liao C, Thanasoula M, Barber P, Hill MA, Tarsounas M (2009) RAD51C facilitates checkpoint signalling by promoting Chk2 phosphorylation. *J Cell Biol* **185**: 587–600
- Bartek J, Lukas J (2003) Chk1 and Chk2 kinases in checkpoint control and cancer. *Cancer Cell* **3**: 421–429
- Bartek J, Lukas J (2007) DNA damage checkpoints: from initiation to recovery or adaptation. *Curr Opin Cell Biol* **19**: 238–245
- Beck H, Nähse V, Larsen MS, Groth P, Clancy T, Lees M, Jørgensen M, Helleday T, Syljuåsen RG, Sørensen CS (2010) Regulators of cyclin-dependent kinases are crucial for maintaining genome integrity in S phase. *J Cell Biol* **188**: 629–638
- Bulavin DV, Higashimoto Y, Demidenko ZN, Meek S, Graves P, Phillips C, Zhao H, Moody SA, Appella E, Piwnicka-Worms H, Fornace AJJ (2003) Dual phosphorylation controls Cdc25 phosphatases and mitotic entry. *Nat Cell Biol* **5**: 545–551
- Buscemi G, Savio C, Zannini L, Miccichè F, Masnada D, Nakanishi M, Tauchi H, Komatsu K, Mizutani S, Khanna K, Chen P, Concannon P, Chessa L, Delia D (2001) Chk2 activation dependence on Nbs1 after DNA damage. *Mol Cell Biol* **21**: 5214–5222
- Busino L, Donzelli M, Chiesa M, Guardavaccaro D, Ganoth D, Dorrello NV, Hershko A, Pagano M, Draetta GF (2003) Degradation of Cdc25A by beta-TrCP during S phase and in response to DNA damage. *Nature* **426**: 87–91
- Canman CE, Lim DS, Cimprich KA, Taya Y, Tamai K, Sakaguchi K, Appella E, Kastan MB, Siliciano JD (1998) Activation of the ATM kinase by ionizing radiation and phosphorylation of p53. *Science* **281**: 1677–1679
- Celli GB, de Lange T (2005) DNA processing is not required for ATM-mediated telomere damage response after TRF2 deletion. *Nat Cell Biol* **7**: 712–718
- Chehab NH, Malikzay A, Appel M, Halazonetis TD (2000) Chk2/hCds1 functions as a DNA damage checkpoint in G1 by stabilizing p53. *Genes Dev* **14**: 278–288
- Chen F, Zhang Z, Bower J, Lu Y, Leonard SS, Ding M, Castranova V, Piwnicka-Worms H, Shi X (2002) Arsenite-induced Cdc25C degradation is through the KEN-box and ubiquitin-proteasome pathway. *Proc Natl Acad Sci USA* **4**: 1990–1995
- Cuadrado M, Martinez-Pastor B, Murga M, Toledo LI, Gutierrez-Martinez P, Lopez E, Fernandez-Capetillo O (2006) ATM regulates ATR chromatin loading in response to DNA double-strand breaks. *J Exp Med* **203**: 297–303
- Denchi EL, de Lange T (2007) Protection of telomeres through independent control of ATM and ATR by TRF2 and POT1. *Nature* **448**: 1068–1071
- di Fagagna FD, Reaper PM, Clay-Farrace L, Fiegler H, Carr P, von Zglinicki T, Saretzki G, Carter NP, Jackson SP (2003) A DNA damage checkpoint response in telomere-initiated senescence. *Nature* **426**: 194–198
- Falck J, Mailand N, Syljuåsen RG, Bartek J, Lukas J (2001) The ATM-Chk2-Cdc25A checkpoint pathway guards against radioreistant DNA synthesis. *Nature* **410**: 842–847
- Garcia-Muse T, Boulton SJ (2005) Distinct modes of ATR activation after replication stress and DNA double-strand breaks in *Caenorhabditis elegans*. *EMBO J* **24**: 4345–4355
- Gatei M, Sloper K, Sorensen C, Syljuåsen R, Falck J, Hobson K, Savage K, Zhou BB, Bartek J, Khanna KK (2003) Ataxia-telangiectasia-mutated (ATM) and NBS1-dependent phosphorylation of Chk1 on Ser-317 in response to ionizing radiation. *J Biol Chem* **278**: 14806–14811
- Guo X, Deng Y, Lin Y, Cosme-Blanco W, Chan S, He H, Yuan G, Brown EJ, Chang S (2007) Dysfunctional telomeres activate an ATM-ATR-dependent DNA damage response to suppress tumorigenesis. *EMBO J* **26**: 4709–4719
- Hickson I, Zhao Y, Richardson CJ, Green SJ, Martin NMB, Orr AI, Reaper PM, Jackson SP, Curtin NJ, Smith GCM (2004) Identification and characterization of a novel and specific inhibitor of the ataxia-telangiectasia mutated kinase ATM. *Cancer Res* **64**: 9152–9159
- Hirao A, Kong YY, Matsuoka S, Wakeham A, Ruland J, Yoshida H, Liu D, Elledge SJ, Mak TW (2000) DNA damage-induced activation of p53 by the checkpoint kinase Chk2. *Science* **287**: 1824–1827
- Hockemeyer D, Daniels JP, Takai H, de Lange T (2006) Recent expansion of the telomeric complex in rodents: two distinct POT1 proteins protect mouse telomeres. *Cell* **126**: 63–77
- Jazayeri A, Falck J, Lukas C, Bartek J, Smith GCM, Lukas J, Jackson SP (2006) ATM- and cell cycle dependent regulation of ATR in response to DNA double-strand breaks. *Nat Cell Biol* **8**: 37–45
- Jin J, Ang XL, Ye X, Livingstone M, Harper JW (2008) Differential roles for checkpoint kinases in DNA damage-dependent degradation of the Cdc25A protein phosphatase. *J Biol Chem* **283**: 19322–19328
- Kastan MB, Bartek J (2004) Cell-cycle checkpoint and cancer. *Nature* **432**: 316–323
- Le Gac G, Estève PO, Ferec C, Pradhan S (2006) DNA damage-induced down-regulation of human Cdc25C and Cdc2 is mediated by cooperation between p53 and maintenance DNA (cytosine-5) methyltransferase 1. *J Biol Chem* **281**: 24161–24170
- Martinez P, Thanasoula M, Munoz P, Liao C, Tejera A, McNees C, Flores JM, Fernandez-Capetillo O, Tarsounas M, Blasco MA (2009) Increased telomere fragility and fusions resulting from TRF1 deficiency lead to degenerative pathologies and increased cancer in mice. *Genes Dev* **23**: 2060–2075
- Maser RS, DePino RA (2002) Connecting chromosomes, crisis, and cancer. *Science* **297**: 565–569
- Matsuoka S, Huang MX, Elledge SJ (1998) Linkage of ATM to cell cycle regulation by the Chk2 protein kinase. *Science* **282**: 1893–1897
- Matsuoka S, Rotman G, Ogawa A, Shiloh Y, Tamai K, Elledge SJ (2000) Ataxia telangiectasia-mutated phosphorylates Chk2 in vivo and in vitro. *Proc Natl Acad Sci USA* **97**: 10389–10394
- Melixetian M, Klein DK, Sorensen CS, Helin K (2009) NEK1 regulates CDC25A degradation and the IR-induced G2/M checkpoint. *Nat Cell Biol* **11**: 1247–1253
- Mendez J, Stillman B (2000) Chromatin association of human origin recognition complex, cdc6, and minichromosome maintenance proteins during the cell cycle: assembly of prereplication complexes in late mitosis. *Mol Cell Biol* **20**: 8602–8612
- Palm W, de Lange T (2008) How shelterin protects mammalian telomeres. *Annu Rev Genet* **42**: 16.11–16.34
- Palm W, Hockemeyer D, Kibe T, de Lange T (2009) Functional dissection of human and mouse POT1 proteins. *Mol Cell Biol* **29**: 471–482
- Peng CY, Graves PR, Thoma RS, Wu Z, Shaw AS, Piwnicka-Worms H (1997) Mitotic and G2 checkpoint control: regulation of 14-3-3 protein binding by phosphorylation of Cdc25C on serine-216. *Science* **277**: 1501–1505
- Potts PR, Yu H (2007) The SMC5/6 complex maintains telomere length in ALT cancer cells through SUMOylation of telomere-binding proteins. *Nat Struct Mol Biol* **14**: 581–590
- Reinhardt HC, Yaffe MB (2009) Kinases that control the cell cycle in response to DNA damage: Chk1, Chk2, and MK2. *Curr Opin Cell Biol* **21**: 245–255
- Sarkar S, Dey BK, Dutta A (2010) MiR-322/424 and -503 are induced during muscle differentiation and promote cell cycle quiescence and differentiation by down-regulation of Cdc25A. *Mol Biol Cell* **21**: 2138–2149
- Shieh SY, Ahn J, Tamai K, Taya Y, Prives C (2000) The human homologs of checkpoint kinases Chk1 and Cds1 (Chk2) phosphorylate p53 at multiple DNA damage-inducible sites. *Genes Dev* **14**: 289–300
- Shiotani B, Zou L (2009) Single-stranded DNA orchestrates and ATM-to-ATR switch at DNA breaks. *Mol Cell* **33**: 547–558
- Shouse GP, Cai X, Liu X (2008) Serine 15 phosphorylation of p53 directs its interaction with B56gamma and the tumor suppressor activity of B56gamma-specific protein phosphatase 2A. *Mol Cell Biol* **28**: 448–456
- Sorensen CS, Syljuåsen RG, Falck J, Schroeder T, Ronnstrand L, Khanna KK, Zhou BB, Bartek J, Lukas J (2003) CHK1 regulates the S phase checkpoint by coupling the physiological turnover and ionizing radiation-induced accelerated proteolysis of Cdc25A. *Cancer Cell* **3**: 247–258
- St Clair S, Giono L, Varmeh-Ziaie S, Resnick-Silverman L, Liu WJ, Padi A, Dastidar J, DaCosta A, Mattia M, Manfredi JJ (2004) DNA damage-induced downregulation of Cdc25C is mediated by p53 via two independent mechanisms: one involves direct binding to the cdc25C promoter. *Mol Cell* **16**: 725–736

- Stott FJ, Bates S, James MC, McConnell BB, Starborg M, Brookes S, Palmero I, Ryan K, Hara E, Vousden KH, Peters G (1998) The alternative product from the human CDKN2A locus, p14 ARF, participates in a regulatory feedback loop with p53 and MDM2. *EMBO J* **17**: 5001–5014
- Takai H, Smogorzewska A, de Lange T (2003) DNA damage foci at dysfunctional telomeres. *Curr Biol* **13**: 1549–1556
- Takizawa CG, Morgan DO (2000) Control of mitosis by changes in the subcellular location of cyclin-B1-Cdk1 and Cdc25C. *Curr Opin Cell Biol* **12**: 658–665
- Tarsounas M, Muñoz P, Claas A, Smiraldo PG, Pittman DL, Blasco MA, West SC (2004) Telomere maintenance requires the RAD51D recombination/repair protein. *Cell* **117**: 337–347
- Tejera A, Stagno d'Alcontres M, Thanasoula M, Martinez P, Liao C, Tarsounas M, Blasco MA (2010) TPP1 is required for TERT recruitment, telomere elongation during nuclear reprogramming, and normal skin development in mice. *Dev Cell* **18**: 775–789
- Thanasoula M, Escandell JM, Martinez P, Badie S, Munoz P, Blasco M, Tarsounas M (2010) p53 prevents entry into mitosis with uncapped telomeres. *Curr Biol* **20**: 521–526
- Tibbetts RS, Brumbaugh KM, Williams JM, Sarkaria JN, Cliby WA, Shieh SY, Taya Y, Prives C, Abraham RT (1999) A role for ATR in the DNA damage-induced phosphorylation of p53. *Genes Dev* **13**: 152–157
- Toledo LI, Murga M, Zur R, Soria R, Rodriguez A, Martinez S, Oyarzabal J, Pastor J, Bischoff JR, Fernandez-Capetillo O (2011) A cell-based screen identifies ATR inhibitors with synthetic lethal properties for cancer-associated mutations. *Nat Struct Mol Biol* **18**: 721–727
- Vousden KH, Prives C (2009) Blinded by the light: the growing complexity of p53. *Cell* **137**: 413–431
- Wu L, Multani AS, He H, Cosme-Blanco W, Deng Y, Deng JM, Bachilo O, Pathak S, Tahara H, Bailey SM, Deng Y, Behringer RR, Chang S (2006) Pot1 deficiency initiates DNA damage checkpoint activation and aberrant homologous recombination at telomeres. *Cell* **126**: 49–62
- Xiao Z, Chen Z, Gunasekera AH, Sowin TJ, Rosenberg SH, Fesik S, Zhang H (2003) Chk1 mediates S and G2 arrests through Cdc25A degradation in response to DNA-damaging agents. *J Biol Chem* **278**: 21767–21773